Advances in Environmental and Life Sciences 1 (2022) 1-14

Contents lists available at Egyptian Knowledge Bank

Advances in Environmental and Life Sciences

journal homepage: https://aels.journals.ekb.eg

# Effect of gold and silver nanoparticles on the detection of Ciprofloxacin in clinical wastewater by europium and terbium complexes

A M Abbas, Z M Anwar, T Elshafaie*, K M Abou Elnour

*Chemistry Department, Faculty of Science, Suez Canal University, 41522, Ismailia, Egypt*

## Abstract

Ciprofloxacin (CIP) was detected by two binary complexes Eu(III)-$(PDCA)_2$ and Tb(III)-$(PDCA)_2$ (PDCA= pyridine 2,6 dicarboxylic acid) in existence and nonexistence of different supports (silver and gold nanoparticles) using spectroscopic luminescence technique. The luminescent complexes were strongly quenched at 615 and 545 nm for europium and terbium complexes respectively, by ciprofloxacin at pH =7.4 in Tris-HCl buffer solution. The detection limits of CIP were 1.76$\mu$M, 1.49 $\mu$M, and 1.06 $\mu$M using Eu(III)-$(PDCA)_2$, Eu(III)-$(PDCA)_2$-AuNPs and Eu(III)-$(PDCA)_2$-AgNPs, respectively. While in the case of Tb(III)-$(PDCA)_2$, Tb(III)-$(PDCA)_2$- Au NPs, and Tb(III)-$(PDCA)_2$-AgNPs, the detection limits of CIP were 2.05 $\mu$M, 1.77 $\mu$M, and 1.46 $\mu$M, respectively. This method of detection showed a good retrieval for CIP identification in hospital wastewater.

*Keywords: luminescent complexes, Ciprofloxacin, nanogold, nanosilver, detection*

*** Corresponding author**

**E-mail address:** taissir.e@yahoo.com (T. Elshafaie)

doi 10.21608/AELS.2021.100473.1000

Received: 11 October 2021, Accepted: 12 December 2021

Published: 14 December 2021

## 1. Introduction

The synthetic fluoroquinolone Ciprofloxacin drug eliminates the bacteria via stopping protein and DNA formation by the interaction with enzymes responsible for reproductions. It is an established medication for many bone joints, cystitis, and respiratory and urinary system infections. It was considered as one of the final used treatment for such infections [1] , so it was widely used.

Gold nanoparticles (AuNPs) and silver nanoparticles (AgNPs) with an exceptional surface behavior (localized surface plasmon resonance (LSPR)) showed unusual optical properties across visible-near-IR areas via changing shape and size. They have numerous applications in all analytical and medical fields [2], [3].

The luminescence probe is one of the most sensitive, easiest, and fastest analytical techniques that may use, however, the one that based on lanthanide's complexes is the preferred as it offers larger Stokes shift, narrow emission, and long lifetimes, particularly europium and terbium ions complexes (in the range of milliseconds). By insertion of metallic nanostructures all optical behavior of the system will be changed, especially fluorescence [4]– [8]. The effect may be increasing in luminescence intensity (metal-enhanced fluorescence) or the opposite action [9]. Nanoparticles surface plasmons may interact or couple with the excitation wavelength used by the fluorophores and alter the energy transfer by increasing or decreasing since it became unified system (NPs–fluorophore) with the same fluorophore spectral behaviors [10]. Furthermore, by exploiting various metal nanoarchitectures to manipulate fluorescence, both increased fluorescence quantum yield and improved photostability can be realized. [11].

Ciprofloxacin was determined using different techniques such as Gas chromatography (GC) [12], [13] , High-performance liquid chromatography (HPLC) [14] , and UV/Vis spectrophotometric method [15] , which are in general long timing methods and tedious preparation of samples that require a specific chemical reagent with a high cost and environmentally harmful as well.

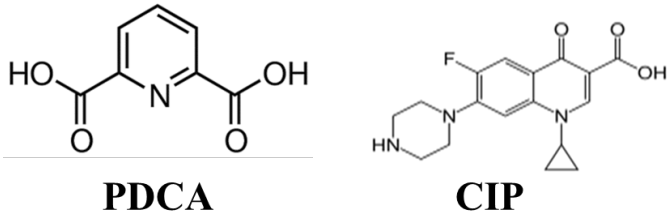


Figure 1: Thestructure of ligand (PDCA) and the drug (CIP)

In this work, fluorescent methods have been used for assessment of ciprofloxacin drug by using luminescent lanthanide complexes, which are considered, simple, sensitive, and highly selective method. The structure of the studied ligand pyridine 2,6 dicarboxylic acid (PDCA) and the drug ciprofloxacin (CIP) are shown in **Figure (1)**.

## 2. Experimental

### *2.1. Apparatus and reagents*

All salts and reagents were of analytical grade and used without any further purification from a standard supplier. Lanthanides salts ($TbCl_3.6H_2O$), ($EuCl_3.6H_2O$), silver nitrate ($AgNO_3$), trisodium citrate ($Na_3C_6H_5O_7$ $.2H_2O$), sodium borohydride ($NaBH_4$), and ciprofloxacin were purchased from EGPI company (www .Info@Egpi.Org.com). Tetrachloroauric acid ($HAuCl_4.4H_2O$) was purchased from Merck.

The Luminescence studies were handled with a JASCO-FP6300 spectrofluorometer outfitted with a 150 W xenon lamp and a 1 cm quartz cell. Jenway 3510 pH meter was used for pH corrections. The UV-Vis spectra were filmed using Lambda 20 (Perkin Elmer) UV-Vis spectrophotometer with a 1 cm quartz cell.

### *2.2. Stock Solutions Preparation*

Stock solutions of ciprofloxacin (1 mM) were prepared in deionized water. For (0.1M) Tris-HCl buffer solution 1.21 g of hydroxy-methyl-aminomethane was dissolved in 80 ml deionized water, the pH was adjusted using concentrated HCl solution (0.5-0.6 ml), then the volume was adjusted

to 100 ml. To obtain a 0.05 M Tris-HCl pH 7.4 solution, dilute 0.1 M Tris-HCl pH 7.4 (1:2) with deionized water. 1.0 % tetrachloroauric acid, 1.0 mM of silver nitrate, 0.05 M trisodium citrate and 2.0 mM of sodium borohydride were prepared by dissolving the appropriate weights in deionized water. Under a dry and freezing (4°C) environment the solutions were stored.

### *2.3. Preparation of working solutions*

The procedure adopted for solution preparation for luminescence measurements includes the preparation of the working probe mixture as follows; 0.2 ml of $EuCl_3.6H_2O$ or $TbCl_3.6H_2O$ stock solutions, 5ml of buffer (pH =7.4), and 0.4 ml of PDCA stock solution were added to a 10 ml volumetric flask. The mixture volume was adjusted to 10 ml with bi-distilled water and incubated for several minutes for constancy.

The fluorescence spectra of Eu(III)-$(PDCA)_2$ and Tb(III)-$(PDCA)_2$ were recorded, then addition of CIP with elevating its concentration gradually with recording the emission spectra after each addition. In an extra step after formation of the probe mixture in 10 ml, 0.1 ml of AuNPs or AgNPs was added, the fluorescence spectra of Eu(III)-$(PDCA)_2$ - AuNPs, Eu(III)-$(PDCA)_2$-Ag NPs, Tb(III)-$(PDCA)_2$ - AuNPs, and Tb(III)-$(PDCA)_2$-AgNPs were recorded in the presence of different concentrations of CIP at excitation wavelength 280 nm and emission wavelengths 614 nm and 545 nm for Eu(III)-$(PDCA)_2$ and Tb(III)-$(PDCA)_2$, respectively. All shoots are repeated at least three times, and the average was taken.

### *2.4. Preparation of Au NPs and Ag NPs*

Tetrachloroauric acid solution 0.016 % was prepared by diluting of 1.0 ml of 1.0 % solution to 62.5 ml; then boiled with stirring after that 10 ml trisodium citrate (0.05 M) was continuously added until the solution transforms splendid red-colored [16]. The concentration of the prepared Au NPs was quantified by UV absorption spectrophotometry using a molar extinction coefficient of $\epsilon = 1.01\times 10^8$ $M^{-1}$ $cm^{-1}$ [17].

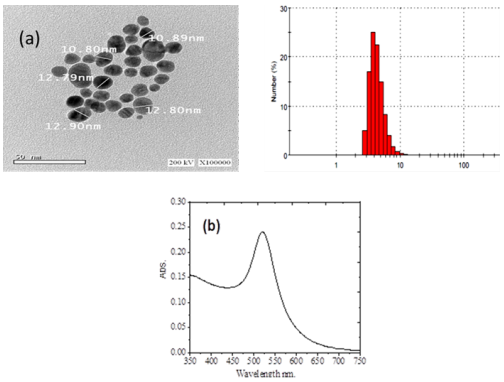


Figure 2: TEMimage (a) and UV-visiblespectrum (b) of Au NPs

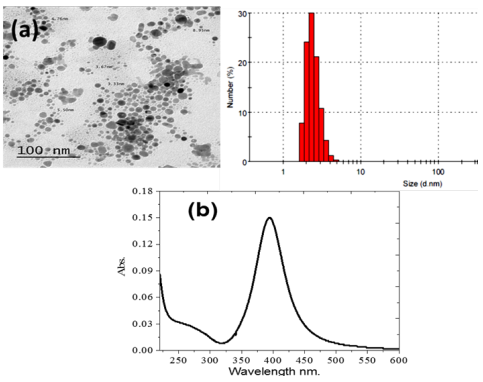


Figure 3: TEMimage (a) and UV-visiblespectrum (b) of AgNPs.

25 ml of $AgNO_3$ solution (1 mM) was added up wisely to 75 ml freshly prepared $NaBH_4$ (2 mM) solution with energetic mixing. The color of the mixture became bright yellow indicates silver ions reduction. The color of the solution indicates that the reduction of silver ions was completed. After 15 minutes of continuous stirring, the stabilizer sodium citrate solution (1.0 wt. %) was added to stabilize the Ag NPs. The Ag NPs colloidal was stirred for extra 30 minutes. All colloidal solutions were stored at $4^o$ C and used for two days only [18]. UV-visible measurements and TEM images were used to confirm the prepared nanoparticles. The concentration of the prepared Ag NPs was quantified by UV absorption using a molar extinction coefficient of $\epsilon = 5.56\times 10^8$ $M^{-1}$ $cm^{-1}$ [19].

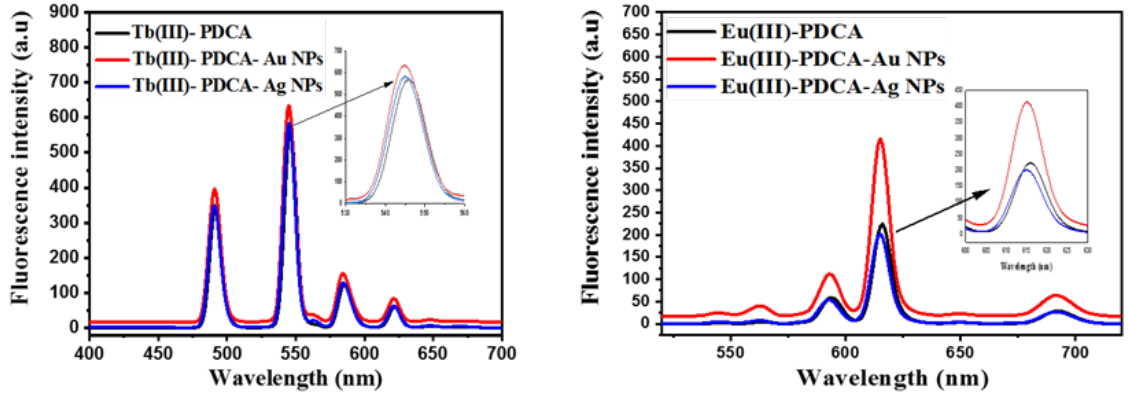


Figure 4: Effect of Au NPs and Ag NPs on the fluorescence spectra of (a)Eu(III)-$(PDCA)_2$, (b) Tb(III)-$(PDCA)_2$ complexes

## 3. Results and discussion

### *3.1. Characterization of nanoparticles*

TEM descriptions of the prepared nanoparticles showed an average particle size of 11 nm and 3 nm for Au NPs and Ag NPs, respectively, according to the scaling depicted in **Figures (2)a** and **( 3)a**. The characteristic plasmonic absorption band of Au NPs and Ag NPs were exhibited at 520 nm and 392 nm, respectively, as in **Figures (2)b** and **(3)b**. The size of the nanoparticles is less than 20 nm, thus it possesses a single surface plasmon band [20].The fluorescence properties and nanoparticles.

The existence of nanoparticles with Eu(III)-$(PDCA)_2$ complex was accompanied by an enhancement in the case of Au NPs and a slight decrease in fluorescence intensity with Ag NPs. In the case of Tb(III)-$(PDCA)_2$, the presence of NPs is accompanied by an enhancement in fluorescence intensity for both additives. In all cases, there was a blue shift in wavelength, as shown in **Figure (4)**.

The presence of nanoparticles with lanthanide complexes were reported to modify the absorption condition [21]. The Nanoparticles can alter the energy transfer to the fluorophores by the interaction between the excited-state fluorophores and surface plasmon electron in the metal NPs [22].

Table 1: Fluorescence intensity of Eu(III)-$(PDCA)_2$ and Tb(III)-$(PDCA)_2$complexes in different buffers.

| Complexes | Buffers | $F^o$ |
|---|---|---|
| Eu(III)-$(PDCA)_2$ | Tris - HCl | 225 |
| | phosphate | 151 |
| | PIPES | 45 |
| | MOPS | 57 |
| | MOPSO | 55 |
| Tb(III)-$(PDCA)_2$ | Tris - HCl | 570 |
| | phosphate | 159 |
| | PIPES | 206 |
| | MOPS | 155 |
| | MOPSO | 239 |

### *3.2. Optimum pH and buffer*

The previous studies indicated that the best pH for PDCA complexes with Eu(III) and Tb(III) was found to be ≈7.5. The presence of Tris buffer was for controlling pH at the required degree [23]. Tris buffer was found to be the best one among several tested buffers, as shown in (**Table 1**) for the fluorescence intensity of the free complexes.

### *3.3. Interaction of CIP with different probes*

The effect of the addition of different concentrations of CIP (2-20 $\mu$M) to the complexes Eu(III)-$(PDCA)_2$ and Tb(III)-$(PDCA)_2$ in the absence and presence of Au NPs and Ag NPs in Tris buffer (1 ml pH= 7.4), showed a quenching in the hypersensitive peak of Eu(III)($^5D_0 \rightarrow {}^7F_2$) at 615 nm

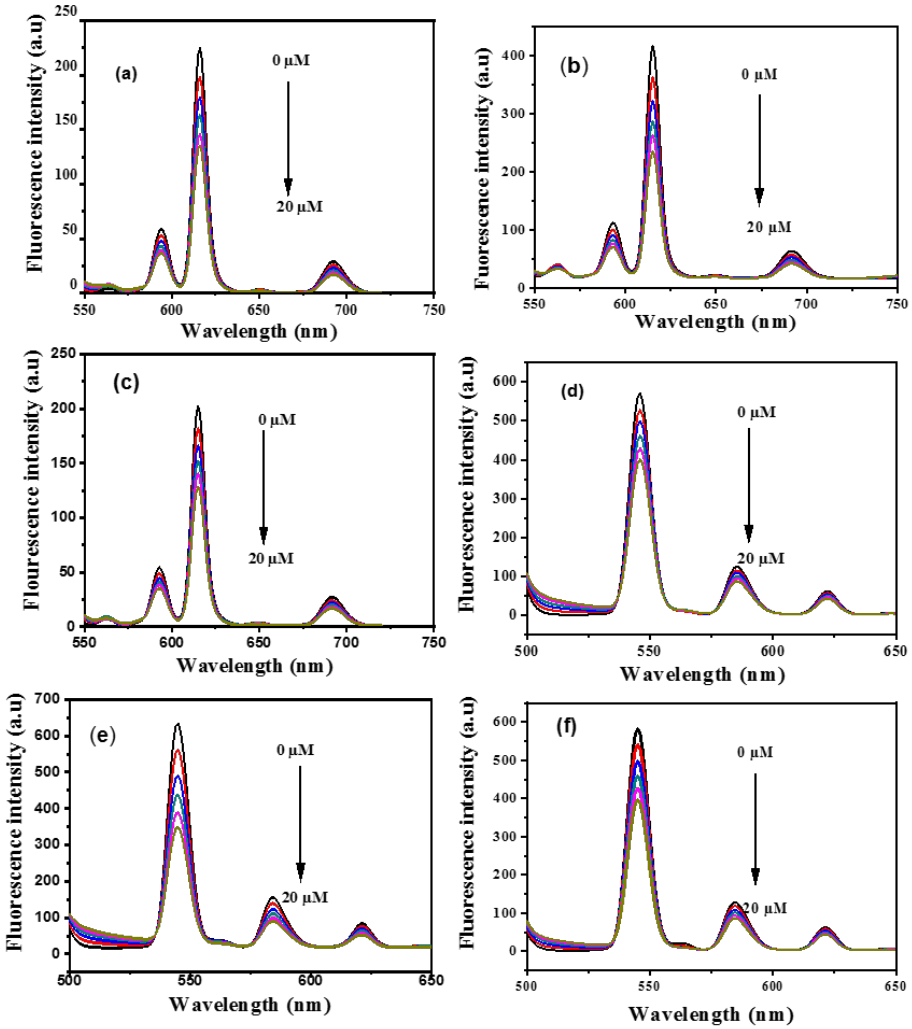


Figure 5: Emission spectra for the interaction of CIP with (a) Eu(III)-$(PDCA)_2$,(b) Eu(III)-$(PDCA)_2$-Au NPs ,(c) Eu(III)-$(PDCA)_2$-Ag NPs,(d) Tb(III)-$(PDCA)_2$ ,(e) Tb(III)-$(PDCA)_2$- Au NPs ,(f)Tb(III)-$(PDCA)_2$-Ag NPs at pH =7.4 using Tris–HCl buffer within aconcentration range: 2$\mu$M to 20 $\mu$M of CIP.

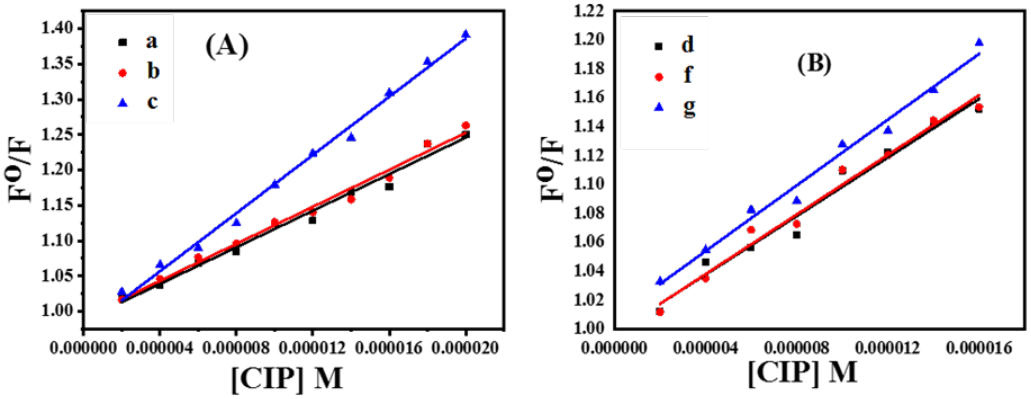


Figure 6: Stern-Volmer equation for the interaction of CIP with [A]: (a)Eu(III)-$(PDCA)_2$ ,(b) Eu(III)-$(PDCA)_2$-AuNPs , (c)Eu(III)-$(PDCA)_2$-AgNPs, and [B]: (d) Tb(III)-$(PDCA)_2$,(f) Tb(III)-$(PDCA)_2$-AuNPs , (g) Tb(III)-$(PDCA)_2$-AgNPs atpH =7.4 using Tris–HCl buffer.

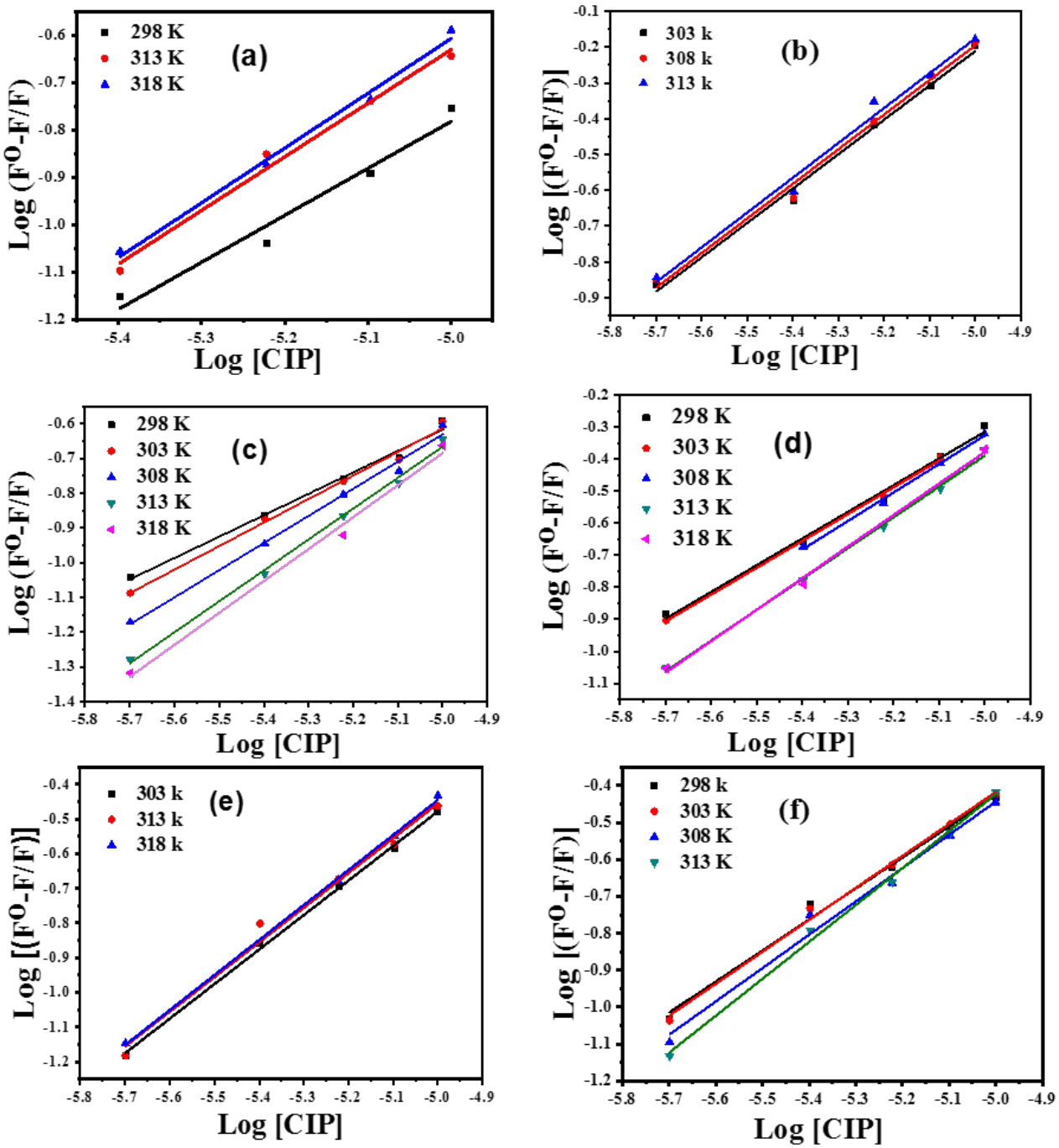


Figure 7: Binding constant plots for CIP with [(a) Eu(III)-$(PDCA)_2$, (b)Eu(III)-$(PDCA)_2$-AuNPs, (c) Eu(III)-$(PDCA)_2$-AgNPs, (d)Tb(III)-$(PDCA)_2$, (e) Tb(III)-$(PDCA)_2$- AuNPs, and (f)Tb(III)-$(PDCA)_2$-AgNPs] complexes at different temperatures.

and that of Tb (III)($^5D_4 \rightarrow {}^7F_5$) at 545 nm in absence and presence of $1.44\times10^{-10}$ M Au NPs and $3.4\times10^{-11}$ M Ag NPs, which confirm the interaction of the drug with the two complexes (**Figure 5**).

### *3.4. Determination of bimolecular quenching constant KSV at different temperatures, LOD, LOQ, and linear range using Stern-Volmer equation.*

Stern-Volmer equation was applied, which represents the relation between CIP concentrations

Table 2: The linear ranges, correlation coefficients, LODs, andLOQs for determination of different CIP using fluorescence measurements viaEu(III)-$(PDCA)_2$ and Tb(III)-$(PDCA)_2$ complexes.

| Probe | Slope (Ksv) $mol^{-1}L$ x $10^4$ | Linear range ($\mu$M) | LOD ($\mu$M) | LOQ ($\mu$M) | $R^2$ |
|---|---|---|---|---|---|
| Eu(III)-(PDCA)2 | 1.29 | 1.76- 19 | 1.76 | 5.86 | 0.980 |
| Eu(III)-(PDCA)2-Au | 1.31 | 1.49-20 | 1.49 | 4.97 | 0.985 |
| Eu(III)-(PDCA)2-AgNPs | 2.06 | 1.06-22 | 1.06 | 3.55 | 0.993 |
| Tb(III)-(PDCA)2 | 1.01 | 2.05-15.97 | 2.05 | 6.83 | 0.969 |
| Tb(III)-(PDCA)2-Au | 1.03 | 1.77-18 | 1.77 | 5.92 | 0.976 |
| Tb(III)-(PDCA)2-AgNPs | 1.14 | 1.46-19.95 | 1.46 | 4.86 | 0.984 |

and the ratio $F^O/F$ for each addition of CIP.

$$\mathbf{F^o/F = 1 + K_{SV}\,[Q]}$$

Where $F^O$ and F are the fluorescence intensities of Eu(III)-$(PDCA)_2$, Eu(III)-$(PDCA)_2$-AuNPs, Eu(III)-$(PDCA)_2$-AgNPs, Tb(III)-$(PDCA)_2$, Tb(III)-$(PDCA)_2$- Au NPs, Tb(III)-$(PDCA)_2$-AgNPs in absence and presence of CIP respectively, as shown in **Figure (6)** which allowed the resolve of changeable parameters such as the limit of detection (3 6 /slope), the limit of quantification (10 6 /slope) [24] , where 6 is the standard deviation of the blank , correlation coefficient ($R^2$), sensitivity, and linear range (**Table (2)**).

All probes have a good sensitivity that is enhanced in presence of NPs. The best detection limits appeared in Ag NPs based complexes. The data obtained proved that these probes could detect and determine CIP drug.

The interaction between ciprofloxacin and different probes is accompanied by fluorescence quenching of the complexes. The quenching process may be static or dynamic quenching. Distinguishing between them can be attached by their different dependence on the temperature and excited state lifetime. The data obtained were recorded in **Table (3)**.

As presented in Table (3), the values of $K_{sv}$ in the case of Eu(III)-$(PDCA)_2$, Eu(III)-$(PDCA)_2$-**AuNPs**, Tb(III)-$(PDCA)_2$-**AuNPs,** and Tb(III)-$(PDCA)_2$-Ag NPs complexes increase directly with temperature increase which means that fluorescence quenching was of the dynamic category where collision takes place firstly

Table 3: Parameters of calibration curves obtained from thedetermination of CIP drug at different temperatures in methanol.

| Complexes parameters | Temperature (K) | Ksv ($mol^{-1}L$) | $R^2$ |
|---|---|---|---|
| Eu(III)-$(PDCA)_2$ | 298 | $1.81\times10^4$ | 0.98987 |
| | 303 | $2.19\times10^4$ | 0.98162 |
| | 313 | $2.33\times10^4$ | 0.99519 |
| | 318 | $2.39\times10^4$ | 1.00212 |
| Eu(III)-$(PDCA)_2$-AuNPs | 303 | $6.30\times10^4$ | 0.99505 |
| | 308 | $6.50\times10^4$ | 0.99531 |
| | 313 | $6.60\times10^4$ | 0.98273 |
| Eu(III)-$(PDCA)_2$-AgNPs | 303 | $2.29\times10^4$ | 0.9585 |
| | 308 | $2.16\times10^4$ | 0.9816 |
| | 313 | $2.13\times10^4$ | 0.9914 |
| | 318 | $2.05\times10^4$ | 0.9593 |
| Tb(III)-$(PDCA)_2$ | 298 | $4.68\times10^4$ | 1.0314 |
| | 303 | $4.62\times10^4$ | 1.0312 |
| | 308 | $4.46\times10^4$ | 1.0296 |
| | 313 | $3.86\times10^4$ | 1.0231 |
| Tb(III)-$(PDCA)_2$-AuNPs | 298 | $3.24\times10^4$ | 0.99833 |
| | 303 | $3.27\times10^4$ | 0.9980 |
| | 308 | $3.31\times10^4$ | 0.98934 |
| | 313 | $3.33\times10^4$ | 0.9874 |
| | 318 | $3.64\times10^4$ | 0.99523 |
| Tb(III)-$(PDCA)_2$-AgNPs | 298 | $3.30\times10^4$ | 0.98577 |
| | 303 | $3.50\times10^4$ | 0.99237 |
| | 313 | $3.80\times10^4$ | 0.99452 |

Table 4: Binding constants and thermodynamicparameters for the interaction of the complexes with CIP.

| Probe | Temperature (K) | Ka (L $mol^{-1}$) | $R_2$ | $\Delta G^0$ (KJ/mol) | $\Delta H^0$ (KJ/ mol) | $\Delta S^0$ (J/mol K) |
|---|---|---|---|---|---|---|
| Eu(III)-$(PDCA)_2$ | 298 | $1.50\times10^4$ | 0.95154 | -23.82 | 91.47 | 387.52 |
| | 313 | $1.10\times10^5$ | 0.98244 | -30.21 | | |
| | 318 | $1.50\times10^5$ | 0.98963 | -31.51 | | |
| Eu(III)-$(PDCA)_2$-AuNPs | 303 | $3.80\times10^4$ | 0.9665 | -26.57 | 18.20 | 147.84 |
| | 308 | $4.30\times10^4$ | 0.9909 | -27.32 | | |
| | 313 | $4.80\times10^4$ | 0.9889 | -28.05 | | |
| Eu(III)-$(PDCA)_2$-AgNPs | 298 | $2.90\times10^2$ | 0.9864 | -14.05 | 133.1 | 494.1 |
| | 303 | $5.90\times10^2$ | 0.98988 | -16.07 | | |
| | 308 | $1.90\times10^3$ | 0.98896 | -19.33 | | |
| | 313 | $6.12\times10^3$ | 0.9942 | -22.69 | | |
| | 318 | $6.14\times10^3$ | 0.98509 | -23.06 | | |
| Tb(III)-$(PDCA)_2$ | 298 | $7.03\times10^3$ | 0.9914 | -21.95 | 67.14 | 297.67 |
| | 303 | $7.29\times10^3$ | 0.9980 | -22.41 | | |
| | 308 | $1.30\times10^4$ | 0.9946 | -24.26 | | |
| | 313 | $2.60\times10^4$ | 0.9968 | -26.45 | | |
| | 318 | $3.40\times10^4$ | 0.9942 | -27.59 | | |
| Tb(III)-$(PDCA)_2$-AuNPs | 303 | $3.16\times10^4$ | 0.9980 | -26.10 | 11.59 | 124.35 |
| | 313 | $3.51\times10^4$ | 0.9830 | -27.24 | | |
| | 318 | $3.97\times10^4$ | 0.9983 | -28.00 | | |
| Tb(III)-$(PDCA)_2$-AgNPs | 298 | $5.93\times10^3$ | 0.98798 | -21.52 | 92.35 | 380.60 |
| | 303 | $8.17\times10^3$ | 0.9938 | -22.69 | | |
| | 308 | $1.17\times10^4$ | 0.9815 | -23.99 | | |
| | 313 | $3.77\times10^4$ | 0.9941 | -27.42 | | |

then a transient complex is formed between the excited state fluorophore and the ground state of the analyte. While in the case of Eu(III)-$(PDCA)_2$-Ag NPs, Tb(III)-$(PDCA)_2$ complexes $K_{sv}$ values dropped down with rising temperature, which confirms the static type of the fluorescence quenching, with forming a ground state non-luminescent complex.

### *3.5. Binding sites and binding constant*

The number of binding positions (n) and binding constants (K) of the contact between the complexes and CIP were calculated by applying the Modified Stern- Volmer equation [25].

$log\frac{F^O-F}{F} = logK + nlogQ$

The numbers of binding sites are calculated from the plot of Log ($F^o$-F)/F versus log [CIP] at different temperatures (**Figure (7)**). The correlation coefficients are more extensive than 0.95, suggesting that the contact between CIP and the complexes comports well in conjunction with the site-binding template. The findings hint that a strong binding force between CIP and the complexes is exhibited. The values of "n" are almost equal to 1, signifying the entity of a single binding site on the complexes for CIP.

### *3.6. $\Delta H$, $\Delta S$, $\Delta G$ calculations for interaction process*

The thermodynamic parameters connected with temperature deviation were evaluated for further illustration of the working forces between Eu(III)-$(PDCA)_2$, Tb(III)-$(PDCA)_2$, and CIP by applying the Van't Hoff equation [26]. **Figure**

Table 5: Effect of coexisting species.

| | Eu(III)-$(PDCA)_2$ | Eu(III)-$(PDCA)_2$-Au NPs | Eu(III)-$(PDCA)_2$-Ag NPs | Tb(III)-$(PDCA)_2$ | Tb(III)-$(PDCA)_2$-Au NPs | Tb(III)-$(PDCA)_2$-Ag NPs |
|---|---|---|---|---|---|---|
| $Na^+$, $Cl^-$ | 1560 | 1190 | 1870 | 2550 | 2040 | 2210 |
| $K^+$, $NO_3$- | 160 | 105 | 110 | 100 | 120 | 140 |
| $Ni^{2+}$, $NO_3^-$ | 1.7 | 0.7 | 1.5 | 3.5 | 1.8 | 3.2 |
| $Ca^{2+}$, $Cl^-$ | 100 | 10.7 | 15 | 80 | 19 | 38 |
| $Cu^{2+}$, $Cl^-$ | 0.7 | 0.5 | 0.7 | 1.5 | 1.5 | 1.5 |
| $Co^{2+}$, $NO_3^-$ | 2.5 | 1.1 | 2 | 2 | 2.7 | 2.8 |
| $NH^{4+}$, Cl- | 200 | 60 | 180 | 120 | 110 | 110 |
| $Mg^{2+}$, $SO_4{}^{2-}$ | 150 | 48 | 70 | 100 | 78 | 90 |
| $Na^+$, $CO_3{}^{2-}$ | 150 | 85 | 130 | 190 | 120 | 150 |
| $Mn^{2+}$, $SO_4{}^{2-}$ | 6 | 1.3 | 2 | 7.5 | 1 | 1.8 |
| $Na^+$, $SO_4{}^{2-}$ | 150 | 53 | 100 | 110 | 60 | 75 |
| $Hg^{2+,}$ $NO_3^-$ | 6.5 | 7 | 9 | 23 | 15 | 16 |
| $Cd^{2+}$, $NO_3^-$ | 0.5 | 0.5 | 0.7 | 2 | 2 | 2.7 |
| $Pb^{2+}$, $NO_3^-$ | 1.5 | 0.9 | 1 | 2.5 | 4 | 4 |
| Glucose | 18 | 11.5 | 16 | 48 | 14 | 28 |

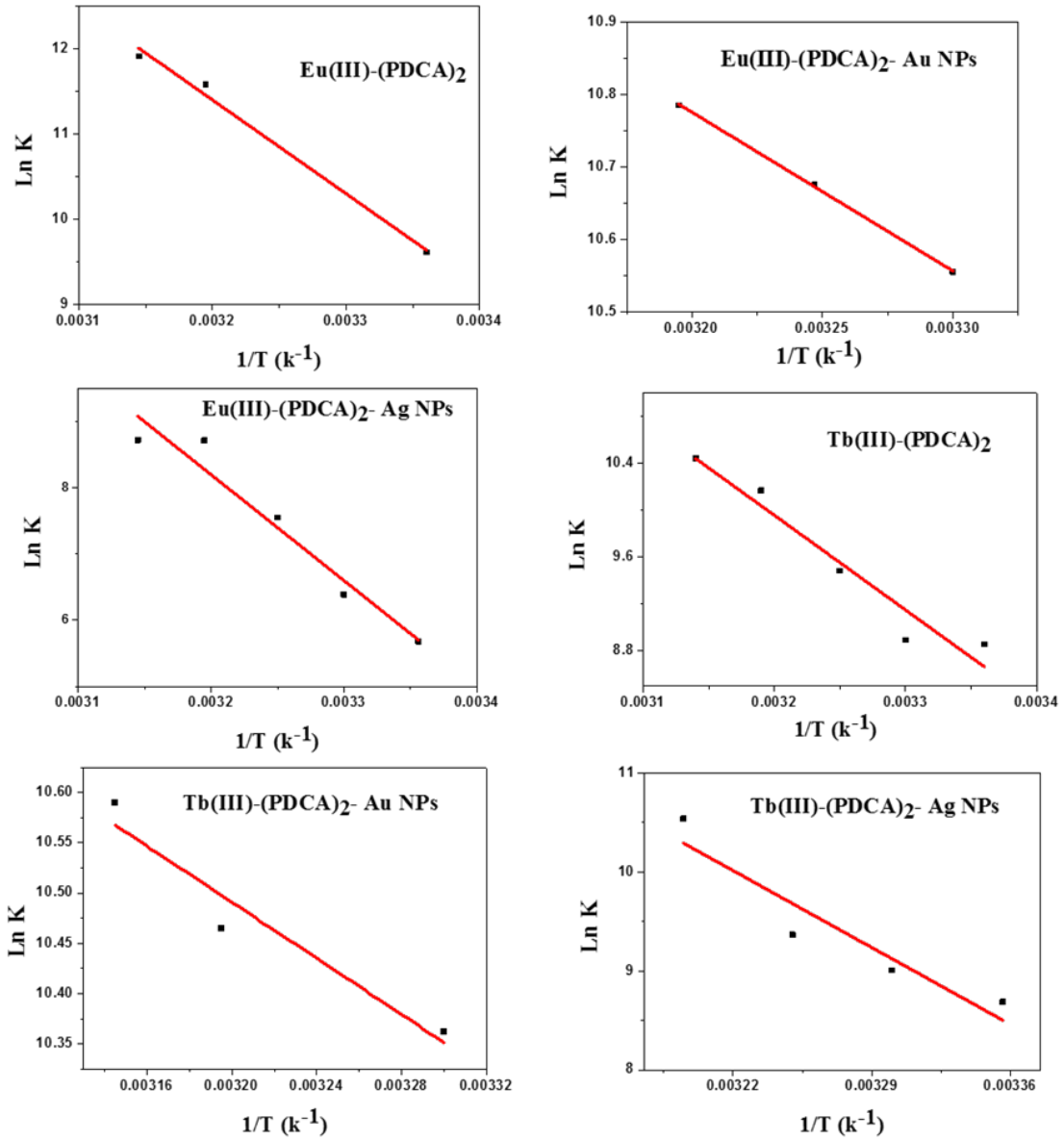


Figure 8: The Van't Hoff plots for CIP with complexes.

Table 6: Characterizationof hospital wastewater an effluent sample*.

| COD ($mgL^{-1}$) | BOD ($mgL^{-1}$) | TDS ($mgL^{-1}$) | DO ($mgL^{-1}$) | pH |
|---|---|---|---|---|
| 31.82 ± 4.6 | 7.87± 0.5 | 349 ± 5.1 | 25.1 ± 3 | 8± 0.2 |

*Repeated three times and average was taken

**(8)** presents the relation between the binding constant (derived from log equation) and 1/K. The calculated binding constant values are collected in a **Table (4)**. The negative $\Delta G^o$ values indicate spontaneous intercalation between CIP and the studied complexes, and the complexation is thermodynamically propitious. The positive values of $\Delta H^o$ indicate that the interaction is endothermic. It was noticed that the values of $\Delta H^o$ are less positive in the case of Eu(III)-$(PDCA)_2$-AuNPs and Tb(III)-$(PDCA)_2$-AuNPs, which indicates that the reaction is more spontaneous than in the presence of Ag NPs or absence of nanoparticles. The positive values of $\Delta H^o$ and $\Delta S^o$ together can be assigned to the hydrophobic

Table 7: Recovering results for CIP in a treated wastewater sample.

| Complexes | Added ($\mu$M) | Found ($\mu$M)* | Recovery % |
|---|---|---|---|
| Eu(III)-$(PDCA)_2$ | 2 | 1.94 | 97 |
| | 6 | 6.1 | 101.7 |
| | 10 | 10.5 | 105 |
| | 16 | 17.5 | 109.4 |
| Eu(III)-$(PDCA)_2$-AuNPs | 2 | 2.01 | 100.5 |
| | 6 | 6.3 | 105 |
| | 10 | 11 | 110 |
| | 16 | 19 | 118.8 |
| Eu(III)-$(PDCA)_2$-AgNPs | 2 | 2.16 | 108 |
| | 6 | 6.8 | 114 |
| | 10 | 11.7 | 117 |
| | 16 | 20 | 125 |
| Tb(III)-$(PDCA)_2$ | 2 | 2.3 | 101.5 |
| | 6 | 6.14 | 102.4 |
| | 10 | 10.2 | 102.3 |
| | 16 | 16.6 | 104 |
| Tb (III)-$(PDCA)_2$-AuNPs | 2 | 1.98 | 99.1 |
| | 6 | 6.1 | 101.7 |
| | 10 | 10.6 | 106 |
| | 16 | 16.7 | 104.4 |
| Tb (III)-$(PDCA)_2$-AgNPs | 2 | 1.96 | 97.8 |
| | 6 | 5.80 | 96.8 |
| | 10 | 10 | 100 |
| | 16 | 16.2 | 101.3 |

interaction which was the most important sponsor to the binding. The enormous amount for the entropy changes as well implies the binding process is largely entropy derived.

### *3.7. Effect of Interferences*

The effect of certain possibly interfering ions that can appear in hospital wastewater was analyzed. They can impinge on the analytical performance as interferents by destroying or improving the luminescence intensity of the scrutinized system. Therefore, the investigation and the deviation in the studied systems' luminescence intensity by 5 % were determined as in **Table (5)**.

### *3.8. Recovery studies of standard additions to CIP in the wastewater*

Our method was applied to determine CIP in hospital wastewater to examine its validity for real sample analysis. The sample was collected from the wastewater effluent of Suez Canal University hospital. The characterization of the hospital wastewater sample was collected in the **Table (6)**. The COD, BOD, TDS, DO, and pH values were determined according to standard methods for examining water and wastewater. The recovery assessments were accomplished by inserting a well-known amount of CIP's standard solution to a wastewater sample. The outcomes attained are demonstrated in **Table (7)**. The recovery values were analyzed by equating the concentration obtained from the spiked samples with additional concentrations. These outputs reveal the likelihood of using Eu(III)-probe or Tb(III)-probe for the analytical assessments of CIP in real wastewater directly from the calibration curve which may provide a benefit for applying our probe in en-

Table 8: Comparing the obtained results with the literature for the determinationof CIP drug.

| Method | LOD (mg/L) | Linear range (mg/L) | Sampling time | Reference |
|---|---|---|---|---|
| HPLC | 0.16 | 4-24 | 30 min | [27] |
| Capillary electrophoresis with capacitively-coupled contactless conductivity detection (CE-C4D) | 1.657 | 16.56–82.84 | 25 min | [28] |
| Batch-injection analysis with amperometry detection (BIA-AMP) | 0.0994 | 0.331-33.14 | 15 min | [29] |
| Square-wave voltammetry using a reduced graphene oxide sensor | 0.075 | 1.97 - 13.14 | 25 min | [30] |
| Eu(III)-$(PDCA)_2$ | 0.65 | 1.96-6.29 | 2 min | This work |
| Eu(III)-$(PDCA)_2$-AuNPs | 0.55 | 1.93-6.63 | 2 min | This work |
| Eu(III)-$(PDCA)_2$ -AgNPs | 0.39 | 1.37-7.29 | 2 min | This work |
| Tb(III)-$(PDCA)_2$ | 0.75 | 2.25-5.29 | 2 min | This work |
| Tb(III)-$(PDCA)_2$-AuNPs | 0.65 | 1.96-5.96 | 2 min | This work |
| Tb(III)-$(PDCA)_2$-AgNPs | 0.54 | 1.90-6.61 | 2 min | This work |

vironmental evaluation. From **Table (8)**, this method is an effective method designed for the detection of CIP since it was simpler, easier, and quicker than the others which are considered time-consuming techniques and have tiresome samples preparation moreover needs certain chemical reagents that are baleful to the environment with a high cost.

## 4. Conclusion

The interaction between CIP and Eu(III)-$(PDCA)_2$ and Tb(III)-$(PDCA)_2$ in the absence and presence of Au NPs and Ag NPs has been investigated with the luminescence technique . It was found that the luminescence of Eu(III)-$(PDCA)_2$ and Tb(III)-$(PDCA)_2$ in the absence and presence of Au NPs and Ag NPs was quenched by CIP under study at pH 7.4, tris-HCl buffer solution. The limit of detection was determined using the Stern Volmer equation, the detection limits of CIP were 1.76$\mu$M, 1.49 $\mu$M, and 1.06 $\mu$M using Eu(III)-$(PDCA)_2$, Eu(III)-$(PDCA)_2$-AuNPs and Eu(III)-$(PDCA)_2$-AgNPs, respectively as a probes. In the case of Tb(III)-$(PDCA)_2$, Tb(III)-$(PDCA)_2$-AuNPs and Tb(III)-$(PDCA)_2$-AgNPs, the detection limits of CIP were 2.05 $\mu$M, 1.77 $\mu$M, and 1.46 $\mu$M, respectively, where LOD values decreased in the presence of Au NPs and Ag NPs. Modified Stern Volmer equation at different temperatures was used to calculate binding constant $K_a$. The thermodynamic parameters $\Delta$H, $\Delta$S, $\Delta$G, were calculated.Hydrophobic interaction was the mechanism of interaction between CIP and the studied complexes. The effect of interfering species was also studied; the method was applied to determine CIP in hospital wastewater showing a reasonable recovery to apply it in environmental assessment.

## References

[1] A. Bhandari, L. I. Close, W. Kim, R. P. Hunter, D. E. Koch, R. Y. Surampalli, Occurrence of Ciprofloxacin, Sulfamethoxazole, and Azithromycin in Municipal Wastewater Treatment Plants, Pract. Period. Hazardous, Toxic, Radioact. Waste Manag 12 (4) (2008) 275–281. doi:10.1061/(ASCE)1090-025X(2008)12:4(275.

[2] S. W. Joo, W. J. Kim, W. S. Yun, S. Hwang, I. S. Choi, Binding of aromatic isocyanides on gold nanoparticle surfaces investigated by surface-enhanced Raman scattering, Appl. Spectrosc 58 (2) (2004) 218–223. doi:10.1366/000370204322842968.

[3] J. E. Millstone, S. J. Hurst, G. S. Métraux, J. I. Cutler, C. A. Mirkin, Colloidal gold and silver triangular nanoprisms, Small 5 (6) (2009) 646–664. doi:10.1002/SMLL.200801480.

[4] J. R. Lakowicz, Radiative decay engineering: Biophysical and biomedical applications, Anal. Biochem 298 (1) (2001) 1–24. doi:10.1006/abio.2001.5377.

[5] T. Gu, J. K. Whitesell, M. A. Fox, Energy transfer from a surface-bound arene to the gold core in ω-fluorenyl-alkane-1-thiolate monolayer-protected gold clusters, Chem. Mater 15 (6) (2003) 1358–1366. doi:10.1021/cm0209867.

[6] G. Liu, Surface-enhanced fluorescence of rhodamine 6G on the assembled silver nanostructures, J. Nanosci. Nanotechnol 11 (11) (2011) 9523–9527. doi:10.1166/JNN.2011.5302.

[7] P. C. Mathias, N. Ganesh, W. Zhang, B. T. Cunningham, Graded wavelength one-dimensional photonic crystal reveals spectral characteristics of enhanced fluorescence, J. Appl. Phys 103 (9) (2008). doi:10.1063/1.2917184.

[8] K. Ray, R. Badugu, J. R. Lakowicz, Metal-Enhanced Fluorescence from CdTe Nanocrystals: A Single-Molecule Fluorescence Study, J. Am. Chem. Soc 128 (2006) 8998–8999.

[9] C. D. Geddes, J. R. Lakowicz, Metal-Enhanced Fluorescence, J. Fluoresc 12 (2) (2002) 121–129. doi:10.1023/A:1016875709579.

[10] K. Aslan, S. N. Malyn, Y. Zhang, C. D. Geddes, Conversion of just-continuous metallic films to large particulate substrates for metal-enhanced fluorescence, J. Appl. Phys 103 (8) (2008). doi:10.1063/1.2905319.

[11] M. Wang, M. Wang, G. Zheng, Z. Dai, Y. Ma, Recent progress in sensing application of metal nanoarchitecture-enhanced fluorescence, Nanoscale Adv 3 (9) (2021) 2448–2465. doi:10.1039/D0NA01050B.

[12] A. N. Ngigi, M. M. Magu, B. M. Muendo, Occurrence of antibiotics residues in hospital wastewater, wastewater treatment plant, and in surface water in Nairobi County, Environ. Monit. Assess 192 (1) 2020–2020. doi:10.1007/s10661-019-7952-8.

[13] L. T. Q. Lien, Antibiotics in Wastewater of a Rural and an Urban Hospital before and after Wastewater Treatment, and the Relationship with Antibiotic Use-A One Year Study from Vietnam, Int. J. Environ. Res. Public Heal 13 (6) (2016) 588–588. doi:10.3390/IJERPH13060588.

[14] C. Rongsayamanont, T. Jaidumrong, D. Bootrak, Removal of antibiotic residues by hospital wastewater treatment facilities in Songkhla, in: 5th International conference on environmental engineering science and management, 2016.

[15] Z. Zhou, J. Q. Jiang, Detection of ibuprofen and ciprofloxacin by solid-phase extraction and UV/Vis spectroscopy, J. Appl. Spectrosc 793 (3) (2012) 459–464. doi:10.1007/S10812-012-9623-1.

[16] J. Turkevich, P. C. Stevenson, J. Hillier, A study of the nucleation and growth processes in the synthesis of colloidal gold, Discuss. Faraday Soc 11 (0) (1951) 55–75. doi:10.1039/DF9511100055.

[17] S. Rahman (2016). doi:10.5038/2326-3652.7.1.4872%0A, [link].
URL http://scholarcommons.usf.edu/ujmm\%0Ahttp://dx.doi.org/10.5038/2326-3652.7.1.4872\%0Ahttp://scholarcommons.usf.edu/ujmm/vol7/iss1/2

[18] D. L. V. Hyning, C. F. Zukoski (1998).

[19] D. Paramelle, A. Sadovoy, S. Gorelik, P. Free, J. Hobley, D. G. Fernig, A rapid method to estimate the concentration of citrate capped silver nanoparticles from UV-visible light spectra, Analyst 139 (19) (2014) 4855–4861. doi:10.1039/c4an00978a.

[20] R. He, X. Qian, J. Yin, Z. Zhu, Preparation of polychrome silver nanoparticles in different solvents, J. Mater. Chem 12 (12) (2002) 3783–3786. doi:10.1039/b205214h.

[21] K. Aslan, I. Gryczynski, J. Malicka, E. Matveeva, J. R. Lakowicz, C. D. Geddes, Metal-enhanced fluorescence: An emerging tool in biotechnology, Curr. Opin. Biotechnol 16 (1) (2005) 55–62. doi:10.1016/j.copbio.2005.01.001.

[22] H. Zhang, C. H. Huang, Oxidative transformation of fluoroquinolone antibacterial agents and structurally related amines by manganese oxide, Environ. Sci. Technol 39 (12) (2005) 4474–4483. doi:10.1021/es048166d.

[23] H. A. Azab, A. Duerkop, Z. M. Anwar, B. H. M. Hussein, M. A. Rizk, T. Amin, Luminescence recognition of different organophosphorus pesticides by the luminescent Eu(III)-pyridine-2,6-dicarboxylic acid probe, Anal. Chim. Acta 759 (2013) 81–91. doi:10.1016/J.ACA.2012.10.045.

[24] D. A. Armbruster, T. Pry, Limit of Blank, Limit of Detection and Limit of Quantitation, Clin. Biochem. Rev 29 (1) (2008) S49–S49.

[25] H. Xu, Q. Liu, Y. Zuo, Y. Bi, S. Gao, Spectroscopic studies on the interaction of vitamin C with bovine serum albumin, J. Solution Chem 38 (1) (2009) 15–25. doi:10.1007/s10953-008-9351-6.

[26] H. A. Azab, I. A. Ibrahim, N. Hassan, A. M. Abbas, H. M. Darwish, Synthesis and photo-physical properties of novel Tb(III) -[Ethyl-4-hydroxy-1-(4-methoxyphenyl)−2-quinolinone-3-carboxylate] complex and luminescence sensitivity towards Malathion and Crotoxyphos pesticides, J. Lumin 192 (Iii) (2017) 376–384. doi:10.1016/j.jlumin.2017.07.007.

[27] N. M. Kassab, A. K. Singh, E. R. M. Kedor-Hackmam, M. I. R. M. Santoro, Quantitative determination of ciprofloxacin and norfloxacin in pharmaceutical preparations by high performance liquid chromatography, Revista Brasileira de Cien-

cias Farmaceuticas/Brazilian Journal of Pharmaceutical Sciences 41 (2005). doi:10.1590/S1516-93322005000400014.

[28] C. A. Clayton, J. W. Hines, P. D. Elkins, Detection Limits with Specified Assurance Probabilities, Anal. Chem 59 (20) (1987) 2506–2514. doi:10.1021/ac00147a014.

[29] R. H. O. Montes, M. C. Marra, M. M. Rodrigues, E. M. Richter, Fast Determination of Ciprofloxacin by Batch Injection Analysis with Amperometric Detection and Capillary Electrophoresis with Capacitively Coupled Contactless Conductivity Detection, Electroanalysis 26 (2014) 432–438. doi:10.1002/elan.201300474.

[30] L. V. Faria, J. F. S. Pereira, G. C. Azevedo, M. A. C. Matos, R. A. A. Munoz, R. C. Matos, Square-wave voltammetry determination of ciprofloxacin in pharmaceutical formulations and milk using a reduced graphene oxide sensor, Journal of the Brazilian Chemical Society 30 (2019). doi:10.21577/0103-5053.20190108.